Minihelix-containing RNAs Mediate Exportin-5-dependent Nuclear Export of the Double-stranded RNA-binding Protein ILF3

Carole Gwizdek, Batool Ossareh-Nazari, Amy Brownawell, Stefan Evers, Ian Macara, Catherine Dargemont

▶ **To cite this version:**

Carole Gwizdek, Batool Ossareh-Nazari, Amy Brownawell, Stefan Evers, Ian Macara, et al.. Minihelix-containing RNAs Mediate Exportin-5-dependent Nuclear Export of the Double-stranded RNA-binding Protein ILF3. Journal of Biological Chemistry, 2004, 279 (2), pp.884-891. 10.1074/jbc.M306808200 . hal-03084591

HAL Id: hal-03084591
https://hal.science/hal-03084591

Submitted on 21 Dec 2020

HAL is a multi-disciplinary open access archive for the deposit and dissemination of scientific research documents, whether they are published or not. The documents may come from teaching and research institutions in France or abroad, or from public or private research centers.

L'archive ouverte pluridisciplinaire **HAL**, est destinée au dépôt et à la diffusion de documents scientifiques de niveau recherche, publiés ou non, émanant des établissements d'enseignement et de recherche français ou étrangers, des laboratoires publics ou privés.

THE JOURNAL OF BIOLOGICAL CHEMISTRY
Vol. 279, No. 2, Issue of January 9, pp. 884–891, 2004
Printed in U.S.A.
© 2004 by The American Society for Biochemistry and Molecular Biology, Inc.

Minihelix-containing RNAs Mediate Exportin-5-dependent Nuclear Export of the Double-stranded RNA-binding Protein ILF3*[S]

Received for publication, June 26, 2003, and in revised form, September 15, 2003
Published, JBC Papers in Press, October 21, 2003, DOI 10.1074/jbc.M306808200

Carole Gwizdek‡§, Batool Ossareh-Nazari‡§, Amy M. Brownawell¶, Stefan Evers‖, Ian G. Macara¶, and Catherine Dargemont‡

From the ‡Institut Jacques Monod, Unité Mixte de Recherche 7592, CNRS, Universités Paris VI et VII, 2 Place Jussieu, Tour 43, Paris 75251 Cedex 05, France, ¶Center for Cell Signaling, University of Virginia, Charlottesville, Virginia 22908, and ‖Hoffmann-La Roche AG, PRPN-G, Building 93/440, 4070 Basel, Switzerland

The karyopherin-related nuclear transport factor exportin-5 preferentially recognizes and transports RNAs containing minihelix motif, a structural cis-acting export element that comprises a double-stranded stem (>14 nucleotides) with a base-paired 5′ end and a 3–8-nucleotide protruding 3′ end. This structural motif is present in various small cellular and viral polymerase III transcripts such as the adenovirus VA1 RNA (VA1). Here we show that the double-stranded RNA-binding protein, ILF3 (interleukin enhancer binding factor 3) preferentially binds minihelix motif. Gel retardation assays and glutathione *S*-transferase pull-down experiments revealed that ILF3, exportin-5, RanGTP, and VA1 RNA assembled in a quaternary complex in which the RNA moiety bridges the interaction between ILF3 and exportin-5. Formation of this complex is facilitated by the ability of both exportin-5 and ILF3 to mutually increase their apparent affinity for VA1 RNA. Using microinjection in the nucleus of HeLa cells and transfection experiments, we show here that formation of the cooperative RanGTP-dependent RNA/ILF3/exportin-5 complex promotes the co-transport of VA1 and ILF3 from the nucleus to the cytoplasm. Exportin-5 thus appears as the first example of a nuclear export receptor that mediates RNA export but also promotes transport of proteinaceous cargo through appropriate and specific RNA adaptors.

Transfer of macromolecules through nuclear pore complexes depends on both structural components of nuclear pore complexes and soluble factors that ensure nuclear transport of a wide diversity of cellular proteins and RNAs. Selectivity of transport is mediated by the recognition of specific signals within the cargoes by specific transport receptors through a direct or adaptor-mediated interaction. Transport receptors interact with nucleoporins thereby mediating docking to and translocation through the nuclear pore complexes. Most of the transport receptors belong to the karyopherin β family (also known as importin β family) and use the GTPase Ran to control cargo association. The asymmetric distribution of the Ran regulatory proteins provides a steep gradient of RanGDP (cytoplasmic)/RanGTP (nuclear) across the nuclear envelope that ensures the directionality of nuclear transport (1, 2). Indeed, nuclear import receptors (importins) bind their cargoes in the cytoplasm in the absence of RanGTP and unload them upon binding to RanGTP in the nucleus. In contrast, export receptors (exportins) require RanGTP to interact with their cargoes in the nucleus, and those export complexes are destabilized by dissociation of RanGTP and GTP hydrolysis in the cytoplasm (3, 4).

Study of nuclear export pathways of diverse viral RNAs has greatly contributed to the identification of cellular factors implicated in nuclear transport processes. In particular, we recently reported nuclear export mechanisms of the adenovirus VA1 RNA (5, 6). This RNA is abundantly transcribed by RNA polymerase III and efficiently exported to the cytoplasm in the late phase of the viral infection. In the cytoplasm, VA1 RNA interacts and inhibits the protein kinase R, a key component of interferon-induced antiviral defense system (7). Analysis of the determinant responsible for the nuclear export of the VA1 RNA led to the identification of a new cis-acting RNA export motif, called minihelix, present not only in VA1 but in a large family of small viral and cellular RNAs transcribed by RNA polymerase III. This structural motif consists in a double-stranded stem (>14 nucleotides) with a base-paired 5′ end and a 3–8-nucleotides protruding 3′ end that can tolerate some mismatches and bends (5). We found that exportin-5 (exp5),[1] a new member of the karyopherin β family, directly interacts, in a RanGTP-dependent manner, with the minihelix motif and mediates nuclear export of the corresponding RNAs (6).

Exportin-5 is a member of the karyopherin β family related to human export receptor CRM1 and the *Saccharomyces cerevisiae* protein, Msn5p/Kap142p. In addition to the minihelix-containing RNAs, exportin-5 has been reported to mediate the nuclear export of ILF3 (interleukin enhancer binding factor 3) and the eukaryotic elongation factor 1A (eEF1A). eEF1A is a GTP-binding protein that interacts with aminoacetylated tRNA and catalyzes their binding to the ribosome. Complex formation between eEF1A and exportin-5 was shown to be strictly dependent on aminoacetylated tRNAs that bridge both proteins (8, 9). Indeed, tRNAs present a highly degenerated minihelix motif able to directly interact with exportin-5, although with a lower affinity than an optimal minihelix structure. Consistently, tRNAs do not represent a preferential cargo for exportin-5 but can use this alternative transport receptor when their own export pathway

* This work was supported by grants from Ensemble contre le Sida, the Association de Recherche contre le Cancer, and the Ligue contre le Cancer. The costs of publication of this article were defrayed in part by the payment of page charges. This article must therefore be hereby marked "*advertisement*" in accordance with 18 U.S.C. Section 1734 solely to indicate this fact.

[S] The on-line version of this article (available at http://www.jbc.org) contains Supplemental Material.

§ Contributed equally to this work.

** To whom correspondence should be addressed. Tel./Fax: 33-1-44276956; E-mail: dargemont@ijm.jussieu.fr.

[1] The abbreviations used are: exp5, exportin-5; eEF1A, eukaryotic elongation factor 1A; dsRBD, double-stranded RNA binding domain; GST, glutathione *S*-transferase; GTPγS, guanosine 5′-3-*O*-(thio)triphosphate; dsRNA, double-stranded RNA; dsRBP, double-stranded RNA-binding protein.

This paper is available on line at http://www.jbc.org

Downloaded from http://www.jbc.org/ at CNRS on December 21, 2020

mediated by exportin-t is deficient (6, 8). ILF3 is a nuclear protein that presenting two double-stranded RNA binding domains (dsRBDs), as well as an RGG domain. It has been shown that exportin-5 interacts, in a RanGTP-dependent manner, with dsRBDs of ILF3 and with dsRBDs from other proteins, including staufen, Spnr, and PKR (10).

To identify factors other than exportin-5 participating in the nuclear export of the VA1 RNA, we attempted to isolate minihelix-binding proteins and identified ILF3 as such a factor. VA1 RNA, ILF3, exportin-5, and RanGTP assembled in a quaternary complex in which VA1 RNA mediates the interaction between ILF3 and exp5. In addition, exportin-5 increases the affinity of ILF3 for VA1, and conversely ILF3 facilitates the interaction between RNA and the export receptor. Finally, the formation of this quaternary complex led to the co-export of both VA1 and ILF3 by exportin-5.

EXPERIMENTAL PROCEDURES

RNA Mutants—VAΔIV, VA-derived mutants, and artificial stems and their *in vitro* transcription have been described previously (5, 6).

Purification of the VA Binding Activity—HeLa nuclear extracts (Computer Cell Culture Center, Seneffe, Belgium) were diluted in binding buffer at a final concentration of 2.5 mg/ml of protein, digested with 100 units/ml of micrococcal nuclease (Worthington) for 15 min at room temperature, and loaded on a single-stranded DNA-agarose column (Amersham Biosciences) equilibrated with binding buffer. The column was washed with binding buffer containing 100 mM NaCl, and elution was performed with binding buffer containing 250 mM NaCl. Eluate (E250; 0.5 mg/ml) was dialyzed against binding buffer. For the affinity selection, VARdm RNA was *in vitro* transcribed in the presence of biotin-16-UTP (Roche Applied Science), and 400 pmol of biotinylated RNA were bound on streptavidin-coated magnetic beads (Dynal) as notified by the manufacturer. After RNA coupling, beads were equilibrated in binding buffer and incubated for 15 min at 4 °C with 0.5 mg of E250 fraction in the presence of 165 μg/ml of poly(C). Beads were washed with binding buffer, and bound proteins were eluted with binding buffer containing 100, 250, or 500 mM NaCl.

Electrophoretic Mobility Shift Assay—Electrophoretic mobility shift assay was performed as described previously (6), excepted for binding buffer (20 mM Hepes pH 7.9, 75 mM KCl, 10 mM β-mercaptoethanol, 0.01% Tween 20, and 10% glycerol) when recombinant proteins were used. When indicated, data from three independent experiments were quantified using ImageQuant 5.1 after scanning gels on a Storm 840 PhosphorImager (Amersham Biosciences).

Expression and Purification of Recombinant Proteins—Expression and purification of His-tagged exportin-5 and GST-ILF3 (404–592) have been described previously (10). His-tagged human ILF3 was expressed from a pET11a plasmid (gift from G. N. Barber (11)). Transformed *Escherichia coli* cells were grown at 37 °C to an A_{600} of 0.6, submitted to cold and chemical shocks, and induced with 0.3 mM IPTG for 6 h at 23 °C prior lysis. The soluble fraction was incubated with 1 mM $CaCl_2$ and 400 units/ml micrococcal nuclease for 12 min at room temperature followed by addition of NaCl to a final concentration of 500 mM and binding to nickel-nitrilotriacetic acid beads (Qiagen) for 1 h at 4 °C. Beads were washed twice with Buffer A (20 mM Hepes, pH 7.9, 500 mM NaCl, 5 mM imidazole, 10% glycerol, 7 mM β mercaptoethanol, 100 μg/ml phenylmethylsulfonyl fluoride, and 5 μg/ml each of leupeptin, pepstatin, and aprotinin), twice for 15 min with Buffer A containing 2 M NaCl, and then in buffer containing 200 mM NaCl. Bound His-ILF3 was eluted in Buffer A plus 500 mM imidazole and dialyzed overnight against Buffer B (20 mM Hepes, pH 7.9, 200 mM NaCl, 10% glycerol, and 7 mM β-mercaptoethanol).

ILF3-associated Bacterial RNA Labeling—Purified recombinant ILF3 containing RNasin was treated with RQ1 RNase-free DNase (200 units/ml; Promega) at 30 °C for 15 min, followed by proteinase K digestion (0.1 μg/μl; Promega) at 37 °C for 30 min. RNA was extracted twice with phenol/chloroform and precipitated. RNAs were then 3′ end-labeled with (5′-^{32}P)-pCp and T4 RNA ligase (PerkinElmer Life Sciences) as described previously (12).

GST-Ran GTPγS Pull Down Assay—GST-Ran was loaded with GTPγS as described elsewhere (13). A mixture containing 1 μM exportin-5, 4 μM GST-Ran GTPγS ± 375 nM VARdm or Mut10 or Mut9 ± 2 μm ILF3 and 2 units/μl RNasin in 40 μl of binding buffer (20 mM Hepes, pH 7.9, 75 mM NaCl, 2 mM magnesium acetate, 0.05% Tween 20, 0.25% ovalbumin, 10 mM β-mercaptoethanol, 5 μM GTPγS, 100 μg/ml phenylmethylsulfonyl fluoride, and 5 μg/ml each of leupeptin, pepstatin, and aprotinin) was incubated for 20 min at 4 °C. Glutathione-Sepharose beads (25 μl; Amersham Biosciences) were then added, and incubation was continued for 40 min. After washing with binding buffer, the beads were resuspended in 40 μl of Laemmli sample buffer. One-fifth of each sample was analyzed by 7% SDS-PAGE and Western blotting. Proteins were detected by monoclonal antibodies against Ran (Transduction Laboratories) and polyclonal antibodies against His tag (Santa Cruz Biotechnology, Inc.) or ILF3 followed by horseradish peroxidase-conjugated anti-mouse or anti-rabbit IgG (Jackson ImmunoResearch Laboratories).

Immunoprecipitation of and Binding to ILF3—Lysates from ~4 × 10^7 HeLa cells were prepared in 100 mM Tris-HCl, pH 7.5, 150 mM NaCl, 1 mM $MgCl_2$, 1 mM $NaVO_4$, 7 mM β-mercaptoethanol, 1% (v/v) Nonidet P-40 plus protease inhibitors (100 μM phenylmethylsulfonyl fluoride, 10 μM leupeptin) and divided into two parts. One portion was treated for 10 min with 1 unit of RNase V1. Endogenous ILF3 was immunoprecipitated from the lysate with 6 μg of anti-ILF3 rabbit antibody attached to protein A-Sepharose beads. Beads were washed extensively in phosphate-buffered saline plus 0.1% Nonidet P-40 and then incubated with binding buffer (150 mM potassium acetate, 20 mM HEPES, pH 7.3, 0.1% Tween, 14 mM β-mercaptoethanol, 0.5% ovalbumin) plus RNase inhibitor (10 units RNasin). The beads were divided equally into tubes and incubated with 1 μg of recombinant exportin-5-His_6 ± 1 μg VARdm RNA ± 10 μg of RanQ69L for 30 min at 4 °C. Beads were then washed with binding buffer, and bound proteins were analyzed by SDS-PAGE and immunoblotting for exportin-5 (rabbit anti-exportin-5 antibody; 1:300) and ILF3 (anti-ILF3; 1:700).

HeLa Cell Microinjections—Microinjections in HeLa cells were performed as described previously (14). *In vitro* transcribed VARdm (22 μM), Mut9 (22 μM), or deionized water were co-injected into the nuclei of HeLa cells with exportin-5-His_6 (0.5 μM) and fluorescent dextran as an injection marker (fluorescein isothiocyanate-dextran 1 mg/ml). Cells were fixed with 4% paraformaldehyde-2% sucrose in phosphate-buffered saline and permeabilized with −20 °C methanol. Endogenous ILF3 was detected using affinity-purified antibody anti-ILF3.2 (2 μg/ml) and Texas Red-conjugated donkey anti-rabbit IgG (Jackson ImmunoResearch Laboratories). DNA was stained with DAPI (10 ng/ml). Images were captured with a ×60 water-immersion objective lens on a Nikon inverted microscope equipped with a Hamamatsu CCD camera. Immunofluorescence data were obtained and processed using Openlab (Improvision) and Adobe Photoshop software.

In Situ Detection of RNAs and Proteins in BHK21 Cells—BHK21 cells were plated on coverslips and co-transfected with the appropriate combination of pVV2VAΔIV (5), pcDNA3.1 ILF3/NFAR-1 (11), and/or pKmyc-exportin-5 (10) plasmids using FuGENE 6 (Roche Applied Science). 20 h after transfection, cells were fixed for 30 min at room temperature with 4% paraformaldehyde in phosphate-buffered saline and permeabilized with 70% EtOH overnight at 4 °C. RNAs were detected by fluorescent *in situ* hybridization as described on the web site Singerlab.aecom.yu.edu, using a Cy3-labeled DNA oligonucleotide probe (Proligo) recognizing a region ranging from nucleotide 24 to nucleotide 63 of VA RNAs. Myc-tagged exportin-5 and ILF3 were subsequently detected by a 30-min incubation with the 9E10 monoclonal antibody to Myc-tag (Roche Applied Science) and affinity-purified anti-ILF3.2 antibody followed by AMCA-conjugated donkey anti-mouse IgG (Jackson ImmunoResearch Laboratories) and fluorescein isothiocyanate-conjugated donkey anti-rabbit IgG (Jackson ImmunoResearch Laboratories), respectively. Images were acquired with a ×100 oil-immersion objective lens on a Leica DMRB epifluorescence microscope equipped with a CCD camera (Princeton) controlled by Metaview software (Universal Imaging Corporation).

Antibodies—Rabbit polyclonal anti-ILF3 antibodies were raised either to *E. coli*-purified His-tagged ILF3 (anti-ILF3.1), kindly provided by G. N. Barber (11), or to amino acids (4–397) of human ILF3 (anti-ILF3.2; Cocalico Biologicals, Reamstown, PA).

RESULTS

ILF3 Interacts with Export-competent RNA Minihelices—To characterize Ran-independent minihelix-binding proteins, nuclear extract from HeLa cells was first passed over a single-stranded DNA column to select nucleic acid-binding proteins. The eluate (E250) was tested for components able to bind VA1 RNA in a electrophoretic mobility retardation assay. To prevent interference in this assay by the La protein, which recognizes 3′ oligo-uridine motifs (15), we used a mutant form of VA1

Downloaded from http://www.jbc.org/ at CNRS on December 21, 2020

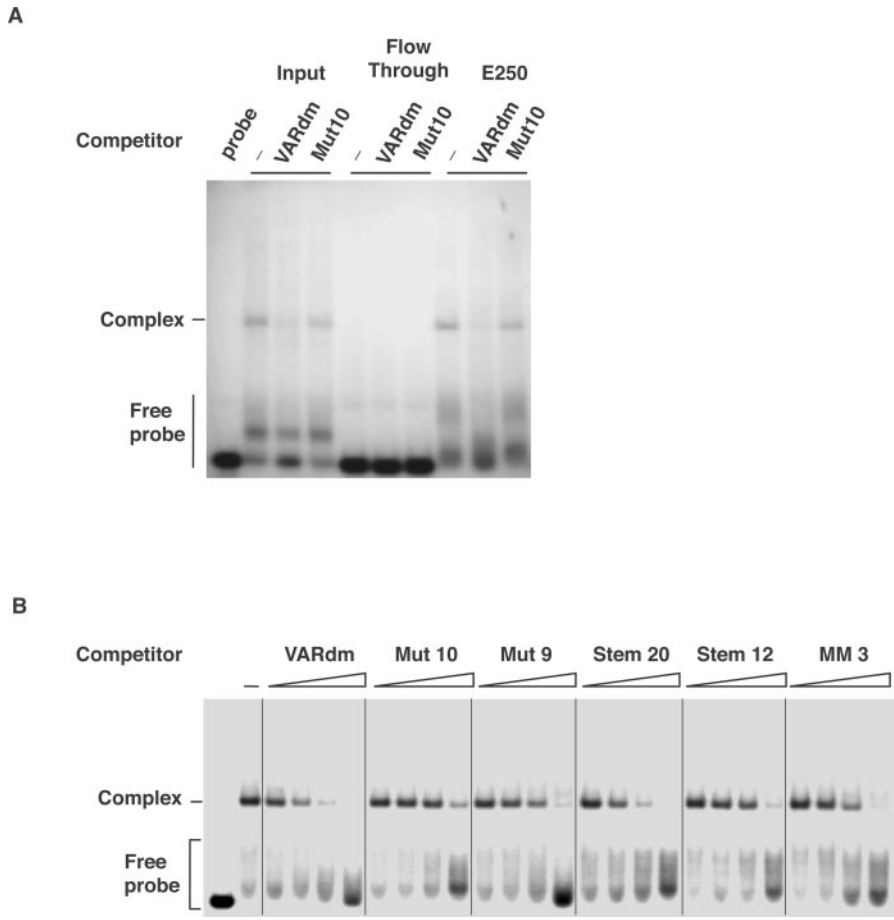

FIG. 1. **Evidence for a VARdm binding activity in HeLa nuclear extracts.** *A*, an electrophoretic mobility retardation assay was performed using a radio-labeled VARdm probe and either total HeLa nuclear extracts (*input*) or single-stranded DNA column flow-through and eluate (*E250*) prepared from HeLa nuclear extracts. Complexes were formed in the absence (−) or in the presence of 5 pmol of the indicated competitor. *B*, an electrophoretic mobility retardation assay was performed using a radio-labeled VARdm probe and single-stranded DNA column eluate (*E250*) prepared from HeLa nuclear extracts. Complexes were formed in the absence (−) or in the presence of increasing amounts (0.25, 1, 2.5, and 10 pmol) of the competitor RNAs indicated *above* the *lanes*. The positions of the free probe and the complex are indicated on the *left*.

(called VARdm) in which this sequence has been modified (6). A VARdm/protein complex was detectable using the E250 eluate (Fig. 1*A*). We then tested the ability of previously described mutant RNAs (6) to compete out the formation of the VARdm/protein complex. Both VA RNA and Stem20, which form an export-competent minihelix structure, efficiently prevented complex formation (Fig. 1*B*). In contrast, mutant RNAs that display mispairing of the 5′ end (Mut9 and MM3), a shorter stem (Stem12), or no stem (Mut10) poorly interfere with complex formation *in vitro* (Fig. 1*B*). The correspondence between the capacity of a given RNA to be exported from the nucleus (5), to inhibit VARdm nuclear export in *Xenopus* oocyte nuclei (6), and to compete with VARdm for formation of the complex, suggested that this complex might be linked to the nuclear export of VARdm.

To identify the VARdm binding activity, a fraction eluted from the single-stranded DNA column (E250) was further purified on a VARdm RNA affinity column. Bound proteins were eluted with increasing salt concentrations and tested for VARdm binding activity using the gel mobility retardation assay (Fig. 2*A*, *right panel*). VARdm binding activity was recovered in the 250 and 500 mM NaCl fractions. Analysis by SDS-PAGE of the proteins eluted under these conditions revealed a correlation between the presence of an 80–90-kDa protein and the VARdm binding activity (Fig. 2*A*, *left panel*, *star*). This protein was excised from the gel and digested *in situ* with trypsin. The resulting peptides were analyzed by mass spectrometry (16), which identified the 80–90-kDa protein as the short form of ILF3 (also called NF90, NFAR-1, MPP4, and DRBP76). ILF3 is a nuclear protein that contains two dsRBD and an RGG domain and that influences gene expression (11, 17–22). Importantly, the RNA/protein complex was dissociated upon addition of anti-ILF3 antibodies whereas mock antibodies had no effect (Fig. 2*B*). This result confirms that ILF3 represents the VARdm binding activity. The formation of an ILF3/VARdm complex was also detected using GST-ILF3 (404–592), a recombinant fusion protein between GST and both dsRBDs of ILF3 (Fig. 2*C*). However no complex could be formed when mutations causing a loss of dsRBD structure were introduced (10) (Fig. 2*C*). Interestingly, the amount of ILF3/VARdm complex measured as a function of GST-ILF3 (404–592) concentration followed a bi-exponential curve suggesting that both dsRBDs could cooperate to bind the same RNA molecule. Although the affinity of GST-ILF3 (404–592) for VARdm is ~50-fold lower than the E250 fraction, the complex was inhibited by VARdm but much less by Mut10 or Mut9 RNAs (Fig. 2, *C* and *D*). Taken together, these results indicate that ILF3 directly interacts with VARdm RNA with the specificity expected for the cellular factor participating to VARdm nuclear export.

ILF3 Forms an RNA-dependent Complex with Exportin-5 and RanGTP—We reported recently that exportin-5 mediates nuclear export of both minihelix-containing RNAs (6) and dsRNA-binding proteins, including ILF3 (10). It has also been shown that interaction between *in vitro* translated ILF3 and exportin-5 was affected upon RNase treatment suggesting that the complex between these proteins was RNA-mediated (8).

To determine whether exportin-5 forms distinct nuclear export complex with dsRNAs and proteins or rather co-transports minihelix-containing RNAs and ILF3, it was first essential to produce RNA-free recombinant ILF3. For this purpose, an His-tagged version of ILF3 produced in *E. coli* was submitted to different salt treatments to extract RNA. RNAs associated with ILF3 prior to and after treatment were purified, 3′ end post-labeled, and analyzed by gel electrophoresis. As shown in Fig. 3*A*, untreated ILF3 was co-purified with small *E. coli* RNAs that were extracted upon treatment with 2 M NaCl. We then

Downloaded from http://www.jbc.org/ at CNRS on December 21, 2020

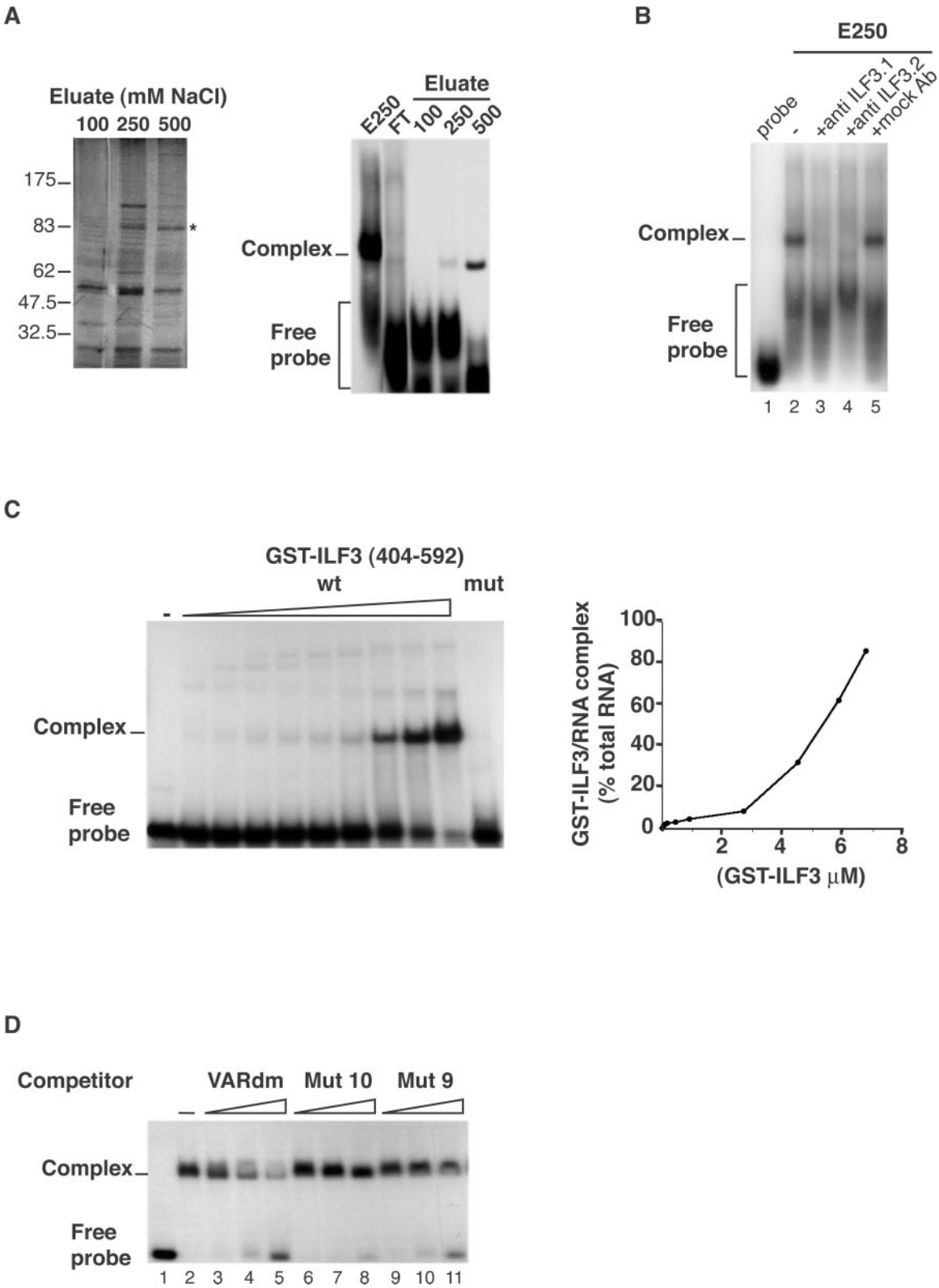

FIG. 2. **Identification of the VARdm binding activity as human ILF3.** *A*, proteins eluted from the single-stranded DNA column (*E250*) were incubated with streptavidin-coated magnetic beads pre-bound to biotinylated VARdm RNAs. Bound proteins were eluted with increasing NaCl concentrations and analyzed by SDS-PAGE and silver staining (*left panel*). The *star* indicates the position of ILF3. Alternatively, E250, flow-through (*FT*), and eluted fractions were assayed in the gel mobility retardation assay on radio-labeled VARdm probe as described in Fig. 2 (*right panel*). *B*, an electrophoretic mobility retardation assay was performed using the E250 fraction in the absence (−) or in the presence of anti-ILF3 or mock antibodies. RNA/protein complexes were formed before addition of antibodies. *C*, an electrophoretic mobility retardation assay was performed on radio-labeled VARdm probe using increasing amounts (from 37 nM to 7 μM) of recombinant GST-ILF3 (404–592) wt or 7 μM mutated GST-ILF3(404–592; F432–559A). The amount of GST-ILF3/RNA complex formed in the different conditions was quantified and expressed as percent of total radiolabeled RNA. *D*, an electrophoretic mobility retardation assay was performed using 9 μM GST-ILF3 (404–592). Complexes were formed in the absence (−) or in the presence of increasing amounts (5, 20, and 50 pmol) of the competitor RNAs indicated *above* the *lanes*.

Downloaded from http://www.jbc.org/ at CNRS on December 21, 2020

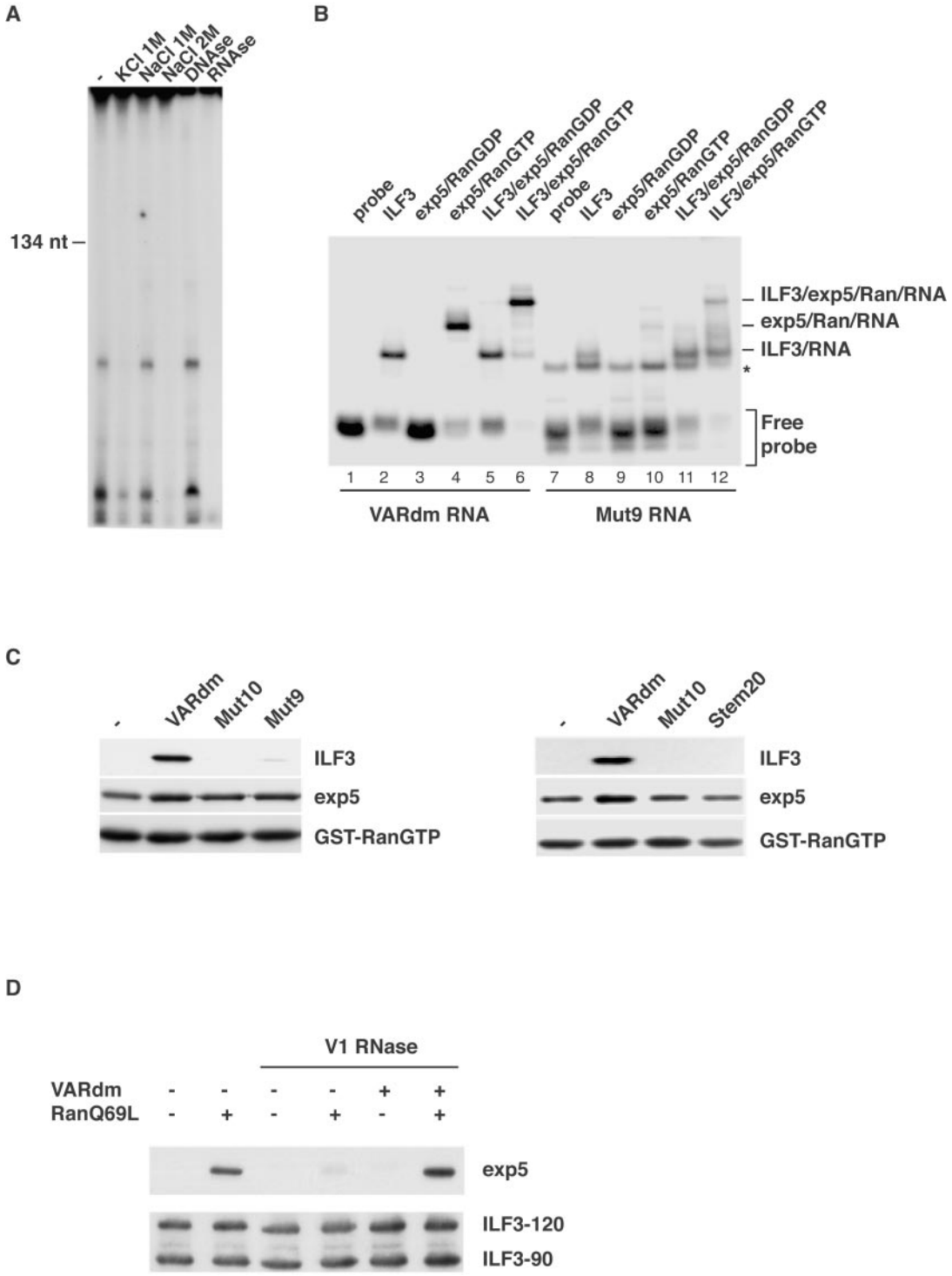

FIG. 3. **ILF3, VA RNA, and exportin-5 form a RanGTP-dependent quaternary complex.** *A*, recombinant His-ILF3 bound on Ni^{2+}-agarose beads was treated with KCl 1 M, NaCl 1 M, or NaCl 2 M before elution as indicated. Purified protein was then treated with proteinase K, and associated RNAs were purified by phenol-chloroform extraction and precipitated. Isolated RNAs were 3′ end-labeled with (5′-^{32}P)-pCp, treated with DNase or RNase when indicated, and resolved by electrophoresis on 8% denaturing polyacrylamide gels. *B*, an electrophoretic mobility retardation assay was performed on radio-labeled VARdm or Mut9 probe using different combinations of recombinant ILF3 (2 μM), exp5 (0.3 μM), Ran GDP (2 μM), or RanQ69L-GTP (2 μM) as indicated. The position of the different RNA/protein complexes formed is indicated. * corresponds to a nonspecific band. *C*, recombinant ILF3 (2 μM), exp5 (1 μM), and GST-RanGTP (4 μM) were incubated in the absence or in the presence of VARdm, Mut10, Mut9, or Stem20 (0.4 μM), and complexes were pulled-down on glutathione-agarose beads. Bound proteins were analyzes by SDS-PAGE and Western blotting using anti ILF3, anti-His, and anti-Ran antibodies. *D*, endogenous ILF3 was immunoprecipitated from HeLa cells with an antibody that recognizes both the 120- and 90-kDa forms of the protein. To destroy any bound RNA, the cell lysates were treated where indicated with V1 RNase. Following digestion, RNase activity was inactivated with RNasin. Recombinant exportin-5-His_6 was added where indicated ± RanQ69L and VARdmRNA.

analyzed the ability of exportin-5 to bind ILF3/VARdm complex by bandshift assay using RNA-free recombinant proteins. As expected, both ILF3 and exportin-5/RanGTP could independently form specific complexes with VARdm whereas they interacted poorly with Mut9 RNA (Fig. 3*B*). Addition of exportin-5 to the ILF3/VARdm complex led to the formation of a RanGTP-

Downloaded from http://www.jbc.org/ at CNRS on December 21, 2020

dependent quaternary complex (Fig. 3*B*, compare *lanes 5* and *6*) that was barely detectable when the RNA 5′ end was mispaired. To determine whether the interaction between exportin-5 and ILF3 within the quaternary complex was direct or rather mediated by the RNA moiety, we tested the ability of ILF3 to bind exportin-5/GST-RanGTP in the absence or in the presence of RNA. This GST pull-down assay clearly revealed that the interaction between ILF3 and exportin-5 required addition of VARdm (Fig. 3*C*). Consistent with gel shift assays, neither Mut10 nor Mut9 were able to mediate this interaction in the same experimental conditions. Interestingly, addition of a minihelix-containing RNA with a shorter stem than VARdm (Stem 20) did not allow the formation of the quaternary complex (Fig. 3*C*). In agreement with data obtained using recombinant ILF3, we found that endogenous ILF3 immunoprecipitated from HeLa cells and treated with RNase VI, which specifically degrades dsRNAs, interacted with exportin-5 in a dsRNA- and RanGTP-dependent manner (Fig. 3*D*). This interaction could not be mediated by tRNA or small interfering RNA (not shown). Together these data clearly indicate that binding of both exportin-5 and ILF3 on the same RNA molecules requires not only a minihelix structure but also a sufficient length of double-stranded RNA likely to avoid any steric hindrance.

The Formation of the VaRdm/ILF3/Exportin-5/RanGTP Quaternary Complex Is Cooperative—To get further insights on the formation of the quaternary complex, the effect of exportin-5 on the ILF3/VARdm interaction was analyzed by gel shift assay using increasing concentrations of ILF3 in the presence or absence of exportin-5. As shown on Fig. 4*A*, 4% of VARdm interacted with ILF3 used at 1 μM in the absence of exportin-5 whereas 40% of VARdm was engaged in the quaternary complex in the presence of exportin-5 and the same concentration of ILF3 (Fig. 4*A*, compare *ILF3/RNA* and *ILF3/exp5/Ran/RNA*). Exportin-5 thus clearly facilitated the binding of ILF3 to VaRdm and decreased the pseudo-K_d by a factor of ~3. Conversely, when the binding of exportin-5 to VARdm and to VARdm/ILF3 were compared using increasing amounts of exportin-5, ILF3 also increased the binding of exportin-5 to VARdm at sub-optimal concentration of exportin-5 (Fig. 4*B*, compare *exp5/Ran/RNA* and *ILF3/exp5/Ran/RNA*). As exportin-5 interacts with VaRdm at a nanomolar range whereas ILF3 binds RNA at a micromolar range, the effect of exportin-5 on the formation of ILF3/VaRdm complex was more obvious. These *in vitro* results clearly show that each partner of this quaternary complex increases the affinity between the two others thus allowing the cooperative formation the ILF3/RNA/exportin-5/RanGTP export complex.

VARdm Stimulates ILF3 Nuclear Export ex Vivo—To evaluate the functional consequences of this RNA-mediated ILF3/exportin-5 interaction, we analyzed the effect of minihelix-containing RNAs on the nuclear export of ILF3 by microinjection experiments. For this purpose, VARdm or M9 RNAs were co-injected with exportin-5 in the nucleus of HeLa cells, and the localization of endogenous ILF3 was assessed by indirect immunofluorescence using anti-ILF3 antibodies and quantified in each condition (Fig. 5, *A* and *B*). Although ILF3 can shuttle between nucleus and cytoplasm (10), more than 90% of endogenous ILF3 was localized, at the steady-state, in the nucleus of non-injected cells or cells microinjected with water or Mut9 (Fig. 5*A*, *panels e* and *h*). In contrast, microinjection of VARdm into the nucleus promoted the shift of a significant fraction of endogenous ILF3 to the cytoplasm (35.7 ± 5.7%; see Fig. 5, *A*, *panel b*, and *B*). Similarly, VARdm and not M9 RNA was able to delocalize from the nucleus to the cytoplasm the GST-GFP-ILF3 (533–640) fusion protein micro-

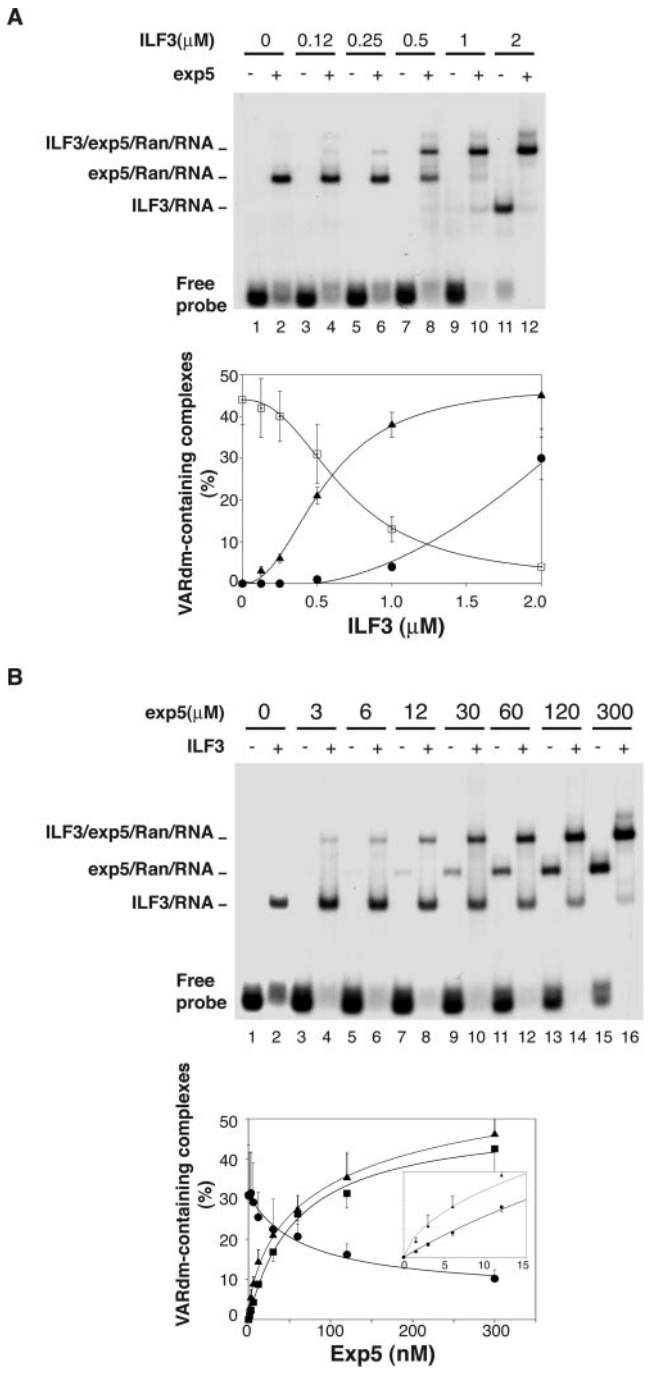

FIG. 4. **VA RNA, ILF3, RanGTP, and exportin-5 form a cooperative complex.** *A*, radio-labeled VARdm-containing complexes were formed in the absence (−) or in the presence (+) of exp5 (300 nM) supplemented with RanQ69L-GTP (1 μM) and increasing concentrations of ILF3. Complexes were analyzed by electrophoretic mobility retardation assay. The position of the different RNA/protein complexes is indicated on the *left*. VARdm-containing complexes were quantified in each condition from three independent experiments (*filled circle*, ILF3/RNA; *filled triangle*, ILF3/exp5/Ran/RNA; *open square*, exp5/Ran/RNA). *B*, radio-labeled VARdm-containing complexes were formed in the absence (−) or in the presence (+) of ILF3 (2 μM) and increasing concentrations of exportin-5 supplemented with RanQ69L-GTP (1 μM). Complexes were analyzed by electrophoretic mobility retardation assay. The position of the different RNA/protein complexes is indicated on the *left*. VARdm-containing complexes were quantified in each condition from three independent experiments (*filled square*, exp5/Ran/RNA; *filled triangle*, ILF3/exp5/Ran/RNA; *filled circle*, ILF3/RNA).

injected into the nucleus of HeLa cells without co-injection of exportin-5 (not shown). These data indicate that VARdm increased the efficiency of ILF3 nuclear export in HeLa cells and

Downloaded from http://www.jbc.org/ at CNRS on December 21, 2020

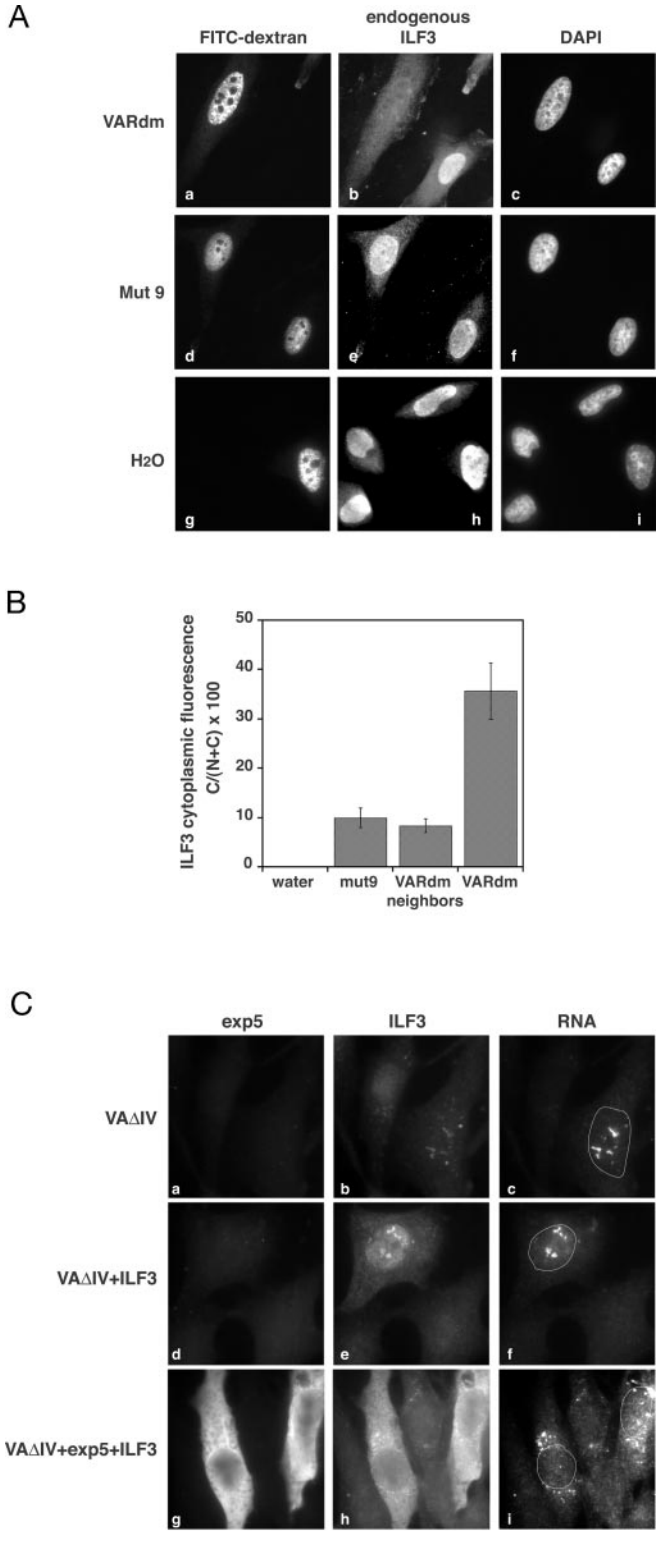

FIG. 5. **ILF3 and VA RNA are co-exported by exportin-5.** *A*, recombinant exp5 (0.5 μM) and VARdm RNA (22 μM), Mut9 RNA (22 μM), or deionized water were injected into the nuclei of HeLa cells using fluorescent dextran as an injection marker. All injected cells were incubated for 2.5 h at 37 °C before fixation. Endogenous ILF3 was detected using the anti-ILF3.2 affinity purified antibody and a Texas Red-conjugated secondary antibody. Nuclei were visualized using DAPI. *B*, mean cytoplasmic fluorescence values for endogenous ILF3 in water-, Mut9-, or VARdm-injected cells or VARdm uninjected nearest neighbor cells were obtained using Openlab (Improvision). All values were corrected for background fluorescence levels and normalized to the cytoplasmic fluorescence levels of water-injected cells. Each *data point* represents the mean cytoplasmic fluorescence obtained from 15 randomly chosen cells. Error is expressed as ±1 S.D. from the mean. The mean cytoplasmic fluorescence of VARdm cells is statistically different by *t* test as compared with that of the water- or Mut9-injected cells and VARdm uninjected nearest neighbor cells. *C*, BHK21 cells were co-transfected with the appropriate combination of plasmids to express VA1 RNA and the indicated proteins (on the *left*). RNAs were detected by fluorescent *in situ* hybridization using a Cy3-labeled DNA oligonucleotide probe (*c*, *f*, and *i*), and proteins were visualized by indirect immunofluorescence using 9E10 monoclonal antibody to detect Myc-tagged exportin-5 (*a*, *d*, and *g*) and an anti-ILF3 antibody (*b*, *e*, and *h*). The localization of the nucleus was drawn in *panels c*, *f*, and *i*.

that endogenous exportin-5 is not a limiting component.

To further confirm that both minihelix-containing RNAs and exportin-5 are required *ex vivo* to efficiently export ILF3, we analyzed the localization of ILF3 in cells expressing a low amount of exportin-5 (Fig. 5*C*). We used a sub-clone of BHK21 cells that do not completely lack exportin-5 but contain a low amount of this protein (see Supplemental Material). In the absence of exogenous ILF3 and exportin-5, VA RNA expressed from transient transfection accumulated in defined nuclear dots (*panel c*). Interestingly, VA RNA was able to de-localize endogenous ILF3 from the nucleoplasm to the same dot structures indicating that VA RNA and ILF3 form a complex in intact cells (*panel b*, compare transfected and untransfected cells). Co-transfection of VA RNA with ILF3 encoding plasmids did not significantly affect the nuclear localization of ILF3 (*panels d–f*) indicating that neither VA RNA nor the weak amount of endogenous exportin-5 alone was sufficient to promote an efficient nuclear export of ILF3 or VA RNA. In contrast, overexpression of both VA RNA and exportin-5 led to a notable increase of both ILF3 and VA RNA in the cytoplasm of transfected cells (*panels g–i*).

Taken together, these data therefore clearly show that minihelix-containing RNAs increase the efficiency of ILF3 nuclear export, likely by promoting the formation of a quaternary ILF3/RNA/exportin-5/RanGTP export complex, and indicate that ILF3 is co-transported with minihelix-containing RNA *in vivo*.

DISCUSSION

Here we identified the dsRNA-binding protein ILF3 as a specific partner for the structural RNA minihelix motif that consists in a double-stranded RNA stem of at least 14 nucleotides, with a base-paired 5′ end and 3–8-nucleotide protruding 3′ end. ILF3 is a nuclear protein presenting two dsRBDs, as well as an RGG domain. Results shown here indicate that both dsRBDs of ILF3 are sufficient to recognize the minihelix structure independently of its sequence and suggest that they could cooperate to bind the same RNA molecule with a micromolar range affinity. Although ILF3 preferentially interacts with minihelix motif, it primarily recognizes dsRNA (17). Indeed high amounts of mutant minihelix compete for the interaction between VA and ILF3, and, in addition, ILF3 also interacts with unspecific dsRNAs such as poly(rI)·poly(rC) (23). Structural analysis of dsRBD from different proteins indicates that the RNA/dsRBD interface is mainly insured by the sugar-phosphate backbone with few base-specific interactions, explaining why dsRBPs recognize a structural motif rather than a consensus sequence (24–27). dsRBDs share a common structure but still exhibit distinct properties. Indeed, characterization of chimeric or truncated proteins shows that dsRBDs are not interchangeable (28). They can exhibit different affinity for dsRNA, cooperate to bind dsRNA (29–31), and are functionally non-equivalent (32, 33). It has been proposed that the combination of several dsRBDs with different properties participates to the substrate specificity of dsRBP. In particular, cleavage affinity assays show that binding of PKR to dsRNAs is mediated by either one or both dsRBDs depending on the ligand, and each dsRDB can recognize different sites on the same RNA

Downloaded from http://www.jbc.org/ at CNRS on December 21, 2020

molecule (34). *In vivo*, ADAR1 and ADAR2 mediate site-specific editing of few cellular RNAs, and both enzymes modify the glutamate receptor B subunit transcript but on distinct adenosines (33, 35, 36). The preference of ILF3 for the minihelix motif can be compared with properties of the RNase Dicer, another dsRBP responsible for processing of dsRNA precursor of miRNAs and small interfering RNAs. Although Dicer is able to initiate processing at internal sites of dsRNA substrates, it cleaves more efficiently dsRNAs at their termini (37).

We recently reported (6) that the nuclear transport factor exportin-5 also interacts with the minihelix motif. However, this high affinity interaction (nM range) is strictly controlled by RanGTP. Here we show that ILF3, VA RNA, and exportin-5 form a RanGTP-dependent quaternary complex. GST pull-down assays using an RNA-free recombinant ILF3 clearly indicate that the VA RNA mediates the interaction between ILF3 and exportin-5. This result is consistent with a recent study (8) showing that the exportin-5/ILF3 interaction was prevented by RNase treatment but contradicts our primary observations. We indeed described a direct and dsRNA-sensitive binding between exportin-5 and dsRBDs (10). The apparent discrepancy was because of co-purification of recombinant ILF3 with *E. coli* RNAs that mediated interaction with exportin-5 and use of dsRNA presenting a long unpaired 5′ end unable to bind exportin-5. Interestingly, a minihelix-containing RNA with a shorter stem than VA (Stem 20) is unable to promote the quaternary complex formation indicating that a minimal dsRNA length is required to bridge exportin-5 and dsRBP, possibly to avoid steric hindrance. In this respect, it should be noted that export efficiency is lower for Stem 20 than for VA RNA (5). Although both exportin-5 and ILF3 preferentially interact with the minihelix structure, it is conceivable that they occupied distinct binding sites on the same RNA to form the quaternary complex.

Exportin-5 promotes nuclear export of the VA RNA and probably mediates transport of viral and cellular RNAs containing such a motif (6). In the present study, micro-injection of VA RNA in the nucleus of HeLa cells or overexpression of both VA RNA and exportin-5 in BHK21 cells induces delocalization of ILF3 from the nucleus to the cytoplasm, likely by allowing the formation of an ILF3/VA/exp5/RanGTP export complex and subsequent VA/ILF3 co-transport. Likewise, it has been proposed that exportin-5 could export tRNA when their own export pathway, involving exportin-t, is deficient and promotes nuclear export of eEF1A through aminoacetylated tRNA (8, 9). Thus, exportin-5 is the first example of a nuclear export receptor that mediates RNA export and drives transport of proteinaceous cargo through an appropriate and specific RNA adaptor. This concept might apply to diverse RNPs, in particular to proteins that associate to mRNAs during their maturation process and could accompany them during exit from the nucleus.

Besides the co-transport of ILF3 and VA RNA, our results raise the question of whether ILF3 could be involved in the export process. We show here that VA is able to interact with exportin-5 or ILF3 alone, but both proteins mutually increase their binding to VA at sub-saturating concentrations. This suggests that ILF3 could act as a facilitating factor in transport, for example by stabilizing the export competent structure of the RNA terminal end. VA presents a 3′ protruding end consisting in an oligouridine stretch, a transcriptional termination signal for polymerase III transcripts, but also as a primary binding site for the La protein that behaves as a nuclear retention factor (38, 39). Mutation of the oligouridine stretch in a random sequence increased the export efficiency of the resulting VA RNA (VARdm) indicating that the oligouridine stretch is not required for transport and rather mediates retention of VA in the nucleus, likely through its interaction with the La protein (6). ILF3 could thus facilitate nuclear export of the VA RNA by displacing the La protein and reducing its nuclear retention. Finally, co-transported ILF3 could protect the terminal end of the VA from cytoplasmic nuclease such as Dicer. According to this hypothesis, miRNA precursors presenting a 30 base-paired long hairpin structure are potential substrates for exportin-5, but the shortness of their terminal stem won't allow interaction with ILF3 and would remain accessible for Dicer processing.

Acknowledgments—We thank G. N. Barber for kindly providing full-length ILF3 constructs and anti-ILF3 antibodies. We thank members of the laboratory and Brigitte Gontero for helpful and stimulatory discussions and M. Rodriguez for critical reading of the manuscript. Special thanks are due to Daniel Roeder (Hoffman-La Roche) for technical assistance in mass spectrometry and E. Bertrand for help in *in situ* hybridization.

REFERENCES

1. Gorlich, D. (1998) *EMBO J.* **17,** 2721–2727
2. Smith, A. E., Slepchenko, B. M., Schaff, J. C., Loew, L. M., and Macara, I. G. (2002) *Science* **295,** 488–491
3. Mattaj, I. W., and Englmeier, L. (1998) *Annu. Rev. Biochem.* **67,** 265–306
4. Ossareh-Nazari, B., Gwizdek, C., and Dargemont, C. (2001) *Traffic* **2,** 684–689
5. Gwizdek, C., Bertrand, E., Dargemont, C., Lefebvre, J. C., Blanchard, J. M., Singer, R. H., and Doglio, A. (2001) *J. Biol. Chem.* **276,** 25910–25918
6. Gwizdek, C., Ossareh-Nazari, B., Brownawell, A. M., Doglio, A., Bertrand, E., Macara, I. G., and Dargemont, C. (2003) *J. Biol. Chem.* **278,** 5505–5508
7. Mathews, M. B., and Shenk, T. (1991) *J. Virol.* **65,** 5657–5662
8. Calado, A., Treichel, N., Muller, E. C., Otto, A., and Kutay, U. (2002) *EMBO J.* **21,** 6216–6224
9. Bohnsack, M. T., Regener, K., Schwappach, B., Saffrich, R., Paraskeva, E., Hartmann, E., and Gorlich, D. (2002) *EMBO J.* **21,** 6205–6215
10. Brownawell, A. M., and Macara, I. G. (2002) *J. Cell Biol.* **156,** 53–64
11. Saunders, L. R., Perkins, D. J., Balachandran, S., Michaels, R., Ford, R., Mayeda, A., and Barber, G. N. (2001) *J. Biol. Chem.* **276,** 32300–32312
12. Mourelatos, Z., Dostie, J., Paushkin, S., Sharma, A., Charroux, B., Abel, L., Rappsilber, J., Mann, M., and Dreyfuss, G. (2002) *Genes Dev.* **16,** 720–728
13. Rexach, M., and Blobel, G. (1995) *Cell* **83,** 683–692
14. Nemergut, M. E., and Macara, I. G. (2000) *J. Cell Biol.* **149,** 835–850
15. Maraia, R. J. (2001) *J. Cell Biol.* **153,** F13–18
16. Fountoulakis, M., and Langen, H. (1997) *Anal. Biochem.* **250,** 153–156
17. Liao, H. J., Kobayashi, R., and Mathews, M. B. (1998) *Proc. Natl. Acad. Sci. U. S. A* **95,** 8514–8519
18. Duchange, N., Pidoux, J., Camus, E., and Sauvaget, D. (2000) *Gene* **261,** 345–353
19. Marcoulatos, P., Avgerinos, E., Tsantzalos, D. V., and Vamvakopoulos, N. C. (1998) *J. Interferon Cytokine Res.* **18,** 351–355
20. Matsumoto-Taniura, N., Pirollet, F., Monroe, R., Gerace, L., and Westendorf, J. M. (1996) *Mol. Biol. Cell* **7,** 1455–1469
21. Patel, R. C., Vestal, D. J., Xu, Z., Bandyopadhyay, S., Guo, W., Erme, S. M., Williams, B. R., and Sen, G. C. (1999) *J. Biol. Chem.* **274,** 20432–20437
22. Reichman, T. W., Muniz, L. C., and Mathews, M. B. (2002) *Mol. Cell. Biol.* **22,** 343–356
23. Langland, J. O., Kao, P. N., and Jacobs, B. L. (1999) *Biochemistry* **38,** 6361–6368
24. Kharrat, A., Macias, M. J., Gibson, T. J., Nilges, M., and Pastore, A. (1995) *EMBO J.* **14,** 3572–3584
25. Bycroft, M., Proctor, M., Freund, S. M., St Johnston, D., Gibson, T. J., Nilges, M., and Pastore, A. (1995) *FEBS Lett.* **362,** 333–336
26. Ryter, J. M., and Schultz, S. C. (1998) *EMBO J.* **17,** 7505–7513
27. Nanduri, S., Carpick, B. W., Yang, Y., Williams, B. R., and Qin, J. (1998) *EMBO J.* **17,** 5458–5465
28. Liu, Y., Lei, M., and Samuel, C. E. (2000) *Proc. Natl. Acad. Sci. U. S. A* **97,** 12541–12546
29. Schmedt, C., Green, S. R., Manche, L., Taylor, D. R., Ma, Y., and Mathews, M. B. (1995) *J. Mol. Biol.* **249,** 29–44
30. Nanduri, S., Rahman, F., Williams, B. R., and Qin, J. (2000) *EMBO J.* **19,** 5567–5574
31. Tian, B., and Mathews, M. B. (2001) *J. Biol. Chem.* **276,** 9936–9944
32. Micklem, D. R., Adams, J., Grunert, S., and St. Johnston, D. (2000) *EMBO J.* **19,** 1366–1377
33. Doyle, M., and Jantsch, M. F. (2003) *J. Cell Biol.* **161,** 309–319
34. Spanggord, R. J., Vuyisich, M., and Beal, P. A. (2002) *Biochemistry* **41,** 4511–4520
35. Bass, B. L. (1997) *Trends Biochem. Sci.* **22,** 157–162
36. Keegan, L. P., Gallo, A., and O'Connell, M. A. (2001) *Nat. Rev. Genet.* **2,** 869–878
37. Zhang, H., Kolb, F. A., Brondani, V., Billy, E., and Filipowicz, W. (2002) *EMBO J.* **21,** 5875–5885
38. Simons, F. H., Rutjes, S. A., van Venrooij, W. J., and Pruijn, G. J. (1996) *Rna* **2,** 264–273
39. Boelens, W. C., Palacios, I., and Mattaj, I. W. (1995) *RNA* (*N. Y.*) **1,** 273–283

Downloaded from http://www.jbc.org/ at CNRS on December 21, 2020

Minihelix-containing RNAs Mediate Exportin-5-dependent Nuclear Export of the Double-stranded RNA-binding Protein ILF3

Carole Gwizdek, Batool Ossareh-Nazari, Amy M. Brownawell, Stefan Evers, Ian G. Macara and Catherine Dargemont

J. Biol. Chem. 2004, 279:884-891.
doi: 10.1074/jbc.M306808200 originally published online October 21, 2003

Access the most updated version of this article at doi: 10.1074/jbc.M306808200

Alerts:
- When this article is cited
- When a correction for this article is posted

Click here to choose from all of JBC's e-mail alerts

Supplemental material:
http://www.jbc.org/content/suppl/2003/10/30/M306808200.DC1

Supplemental material:
http://www.jbc.org/content/suppl/2003/10/30/M306808200.DC2

This article cites 39 references, 25 of which can be accessed free at
http://www.jbc.org/content/279/2/884.full.html#ref-list-1

Downloaded from http://www.jbc.org/ at CNRS on December 21, 2020

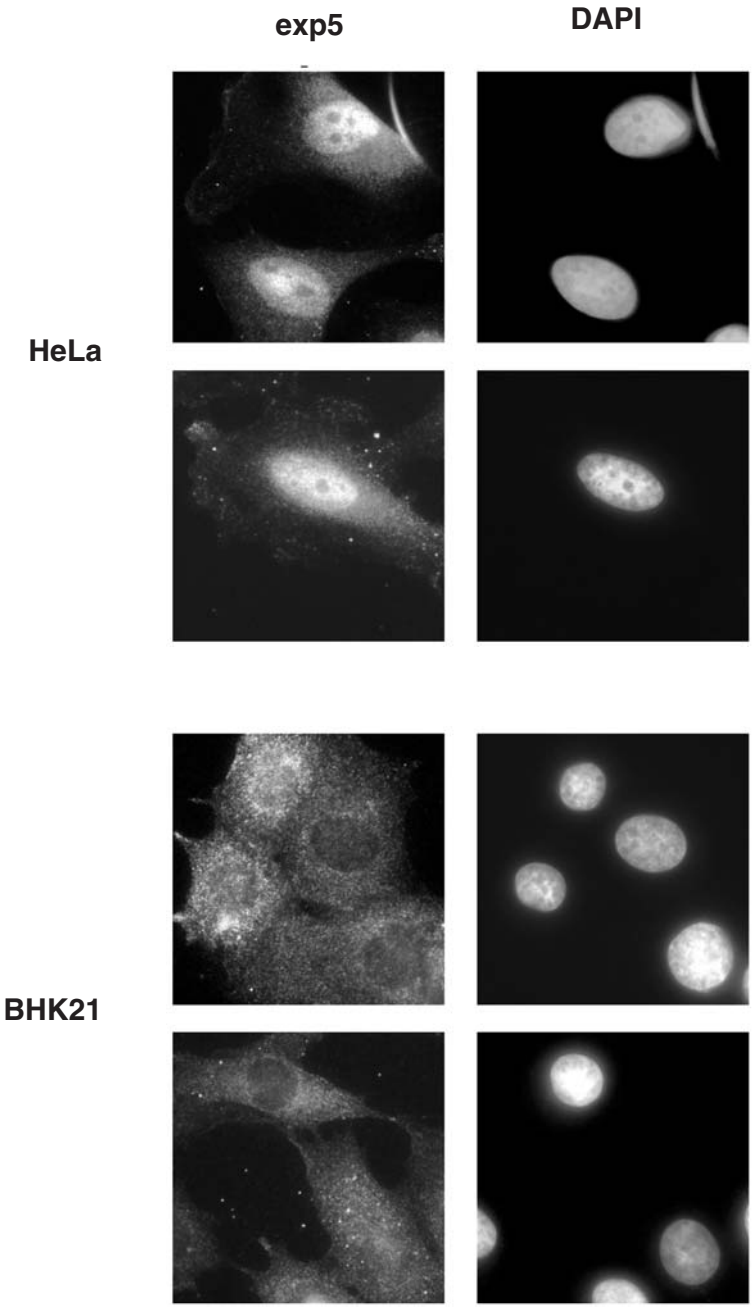
exp5
DAPI
HeLa
BHK21

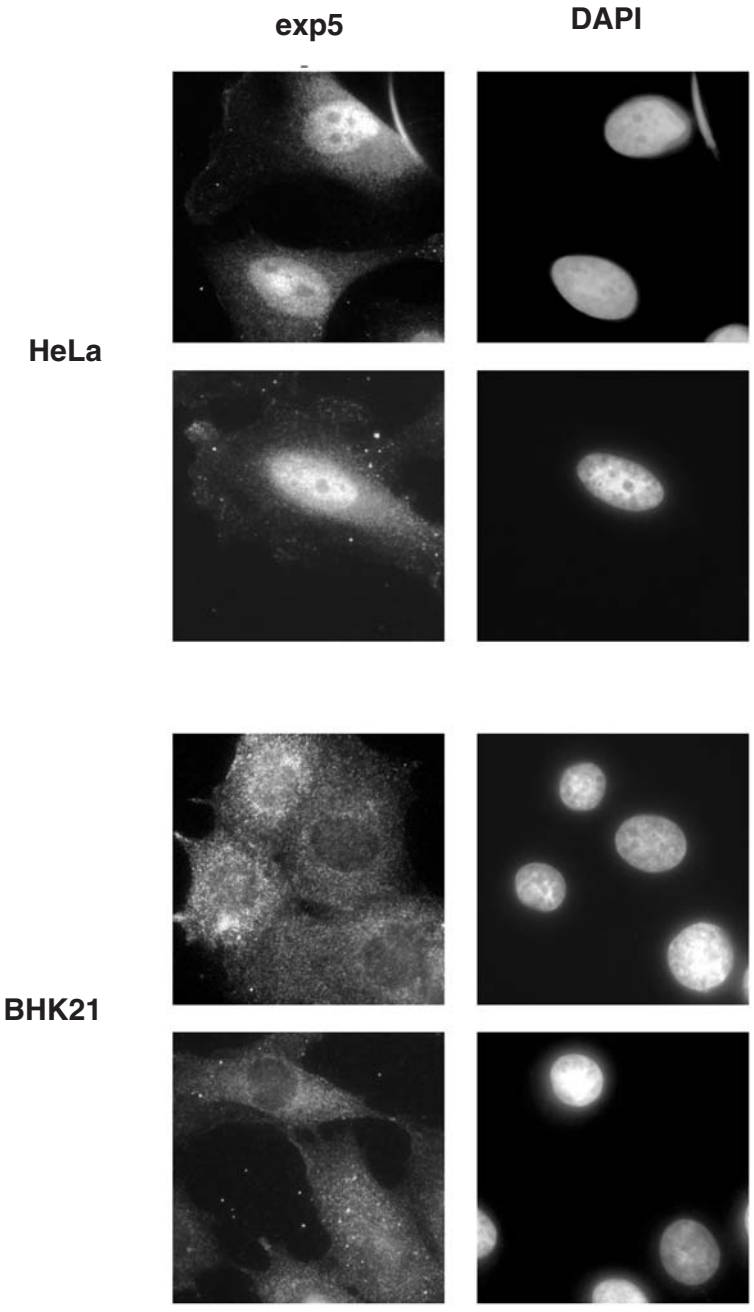
exp5
DAPI
HeLa
BHK21